Calhoun: The NPS Institutional Archive

DSpace Repository

Theses and Dissertations	1. Thesis and Dissertation Collection, all items

1972

An optical apparatus to determine the effect of turbulence on the modulation transfer function of the atmosphere.

Hildebrand, Wayne Thompson.

http://hdl.handle.net/10945/16284

This publication is a work of the U.S. Government as defined in Title 17, United States Code, Section 101. Copyright protection is not available for this work in the United States.

Downloaded from NPS Archive: Calhoun

http://www.nps.edu/library

Calhoun is the Naval Postgraduate School's public access digital repository for research materials and institutional publications created by the NPS community. Calhoun is named for Professor of Mathematics Guy K. Calhoun, NPS's first appointed -- and published -- scholarly author.

Dudley Knox Library / Naval Postgraduate School
411 Dyer Road / 1 University Circle
Monterey, California USA 93943

AN OPTICAL APPARATUS TO DETERMINE THE EFFECT OF TURBULENCE ON THE MODULATION TRANSFER FUNCTION OF THE ATMOSPHERE

Wayne Thompson Hildebrand

Library
Naval Postgraduate School
Monterey, California 93940

NAVAL POSTGRADUATE SCHOOL
Monterey, California

THESIS

AN OPTICAL APPARATUS TO DETERMINE

THE EFFECT OF TURBULENCE

ON THE

MODULATION TRANSFER FUNCTION OF THE ATMOSPHERE

by

Wayne Thompson Hildebrand

Thesis Advisor: E. C. Crittenden, Jr.

December, 1972

Approved for public release; distribution unlimited.

Library
Naval Postgraduate School
Monterey, California 93940

An Optical Apparatus to Determine the Effect of Turbulence on the Modulation Transfer Function of the Atmosphere

by

Wayne Thompson Hildebrand
Lieutenant Commander, United States Navy
B. S., United States Naval Academy, 1959

Submitted in partial fulfillment of the
requirements for the degree of

MASTER OF SCIENCE IN PHYSICS

from the
NAVAL POSTGRADUATE SCHOOL
December, 1972

Library
Naval Postgraduate School
Monterey, California 93940

ABSTRACT

An apparatus was designed and constructed to determine the effect of atmospheric turbulence on the modulation transfer function (MTF) of the atmosphere. A reflecting telescope and reticle system provided optical information in the visible region to a silicon photodiode detector which was responsive from .35 micron to 1.1 microns. The output of the detector was processed to measure irradiance modulation from a target of known spatial frequency. The modulation transfer function of the atmospheric transmission medium and the optical system was measured under calm conditions and conditions of turbulence on a 270 meter round trip path through a building corridor. The optical apparatus described was capable of detecting, in the visible range, the degrading effect of turbulence on MTF. All reflective optics were used so that the visual through 10 micron range can be covered with use of different detectors.

TABLE OF CONTENTS

LIST OF ILLUSTRATIONS

DEDICATION

This thesis is dedicated to the Honorable Patrick J. Hillings, former congressman from California, who made it all possible; and whose faith and support have not been forgotten.

ACKNOWLEDGEMENT

The author wishes to express his sincerest appreciation and gratitude to Mr. Robert Moeller of the technical staff, Naval Postgraduate School, for his time, effort, and many worthwhile suggestions and assistance in the design, construction and alteration of the optical apparatus used throughout the research; and to Mr. Kenneth Smith, also of the technical staff, for his assistance with the electronic instrumentation used.

I. BACKGROUND

The development of the laser and subsequent investigation has led to the application of this device to highly directional communications and has focused attention on the problems involving the properties of the atmosphere as a propagating medium. One particular problem that must be thoroughly investigated is the effect of atmospheric turbulence on the spatial and temporal modulation of such a beam as it is received at the terminal end of such a communications system.

Until recently it was thought that microturbulence over the land was much greater than over water. However, at the October, 1972 meeting of the Optical Society of America in San Francisco, California, it was brought out that the reverse is true. It is now a recognized fact that turbulence effects over water are a big problem and may be a limiting factor in over-water optical communications. Temperature variations, humidity gradients over water, and the correlation cross product are highly affected by over-water turbulence.

Recognizing this situation, it is apparent that a technique capable of evaluating the effect of turbulence on spatial modulation, or 'seeing' of an over-water system would be of value. With this in mind an apparatus was constructed that would provide information on the modulation transfer function of the atmosphere. Such a device, described in this thesis, when used in conjunction with a system that will measure atmospheric turbulence variations, will assist in making such evaluations.

II. THEORY

A. OPTICAL SYSTEM LIMITATIONS

No image formed by any optical system will be an exact representation of the object. The image quality will be a function of at least four considerations: 1. Ray abberations in the design of the system; 2. Manufacturing inaccuracies in the assembly of the system; 3. Focusing misadjustment by the operator; and 4, the inherent diffraction, or light-dark fringing or smearing of the shadow edge, caused by the wave nature of light.

In a scanning optical system other considerations will affect the quality of the image as well as the four mentioned above. One of these is the responsivity time constant, or the time that it takes for the system to reach 63 per cent, $(1 - 1/e)$ of its final value after a change in the irradiance. This is a function of the type of material used in the detector and of the bandwidth of the entire scanning system. Another consideration is the signal-to-noise ratio of the system. This is a function of the detectivity, D, of the detector. Detectivity is the inverse of the noise equivalent power (NEP) of the detector.

$$D = \frac{1}{NEP} = \frac{v_s}{H\, A_d\, v_n} \qquad (1)$$

H = Irradiance on detector

v_s = RMS value of source signal

v_n = RMS value of noise signal

A_d = Area of detector

NEP is the radiant flux necessary to give an output signal equal to the detector noise. The term detectivity, which is a parameter of the detector itself, has been challenged as a good parameter for a system

as a whole. Different equipment will have differing operational and constructional characteristics and cannot be rationally compared. It has been suggested that a better parameter for comparison of detectional ability, and thus an indication of the signal-to-noise ratio, is the parameter, D* (dee-star.) D* includes the bandpass frequency of the system, Δf, and 'normalizes' detectional ability for all systems. The value for D* is;

$$D^* = \frac{(\Delta f \, A_d)^{\frac{1}{2}}}{NEP} \tag{2}$$

so, substituting (1) and simplifying,

$$D^* = \frac{\Delta f^{\frac{1}{2}} \, v_s}{H \, A_d^{\frac{1}{2}} \, v_n} \tag{3}$$

Thus it is evident that signal-to-noise ratio, which is dependent on the detecting ability of the equipment is affected by the bandwidth, the inherent noise of the system, and the physical size of the detector.

All of the items discussed above are integral to the equipment under study. However the transmitting medium, in this case the atmosphere, also plays a part in determination of the image quality. Instabilities, (turbulence,) and the atmospheric scattering and absorption all tend to degrade image quality. This thesis will not be concerned with the real and considerable effects of the latter two items. The contrast of the image of degraded quality is reduced. Reduction in contrast increases with the spatial frequency of the object.

B. MODULATION AND THE MODULATION TRANSFER FUNCTION

The science of optics has been developed as a means to transfer information, or as a means of communication. The communications involved may be active, as in the case of visual signalling via a laser system, or

it may be passive, as in the observation of a specimen under a microscope. But it is, nevertheless, communication or a transfer of information. For this reason it is not surprising to find many terms borrowed from the field of communications engineering. Included in these are two terms of particular interest to the project – modulation, and transfer functions, in this case the modulation transfer function (MTF.)

Modulation, M, is a comparative parameter used when one is concerned with the irradiance of a periodic signal. It is defined as the difference between the maximum irradiance, H_{max}, and the minimum irradiance, H_{min}, divided by the sum of the maximum irradiance and the minimum irradiance; i.e.

$$M = \frac{H_{max} - H_{min}}{H_{max} + H_{min}} \tag{4}$$

Thus the parameter M is the ratio of the variation in irradiance to the average irradiance.

The modulation transfer function describes the ability of any element of an optical system to transfer information. As with other transfer functions MTF is a ratio of output to input. In this case MTF is the ratio of the output modulation to input modulation; or, more exactly, the ratio of the spatial modulation of the image, M_i, to the spatial modulation of the object, M_o,

$$MTF = \frac{M_i}{M_o} \tag{5}$$

Since information can be transferred in a modulated signal only when the signal does, in fact, vary, it is clear that MTF will equal zero when M_i equals zero or H_{max} equals H_{min}. In an optical sense this occurs when no difference can be detected between two unlike shadings; in other words

the system 'sees' what, to it, is a solid, unvarying shade, like the central portion of a large flat wall. Thus it is taken that when resolution of a target is lost MTF equals zero.

In many cases the light available will not be spatially modulated at a single frequency, but will consist of a frequency spectrum, G (irradiance as a function of spatial frequency.) In this case:

$$MTF = \frac{G_i}{G_o} \tag{6}$$

In the case of coherent light, (light produced by lasers,) it is necessary to consider both the irradiance and the phase of the spectrum. In this case:

$$MTF = \left|\frac{G_i}{G_o}\right| \tag{7}$$

(Disregarding imaginary components and considering real components of the spectrum only.)

The MTF curve in most common usage is the plot of MTF versus spatial frequency, and is normalized to 1.0 at zero spatial frequency.

1. MTF of a Coherent System

A point source object at infinity, imaged by a concave mirror produces a diffraction pattern that is the Fourier transform of the mirror aperature. If the aperature is called the pupil function, P, and the diffraction function is called the point spread function, h, then;

$$h = \mathfrak{F}\{P\} \tag{8}$$

A target, or object, of an image system can be considered to consist of a series of point sources. The image of the target is the summation of the diffraction patterns of each point source in the target. Or, another way of describing the image function, U_i, is as the convolution of the object function, U_o, with the point spread function; i.e.

$$U_i = h * U_o \tag{9}$$

The object spatial frequency spectrum, G_o, is the Fourier transform of the object function, U_o; i.e.

$$G_o = \mathfrak{F}\{U_o\} \tag{10}$$

Similarly the image spatial frequency spectrum, G_i, is the Fourier transform of the image function, U_i; i.e.

$$G_i = \mathfrak{F}\{U_i\} \tag{11}$$

Thus, since

$$U_i = h * U_o \tag{9}$$

then

$$\mathfrak{F}\{U_i\} = \mathfrak{F}\{h * U_o\} \tag{12}$$

Substituting (11)

$$G_i = \mathfrak{F}\{h * U_o\} \tag{13}$$

Applying the convolution theorem

$$G_i = \mathfrak{F}\{h\}G_o \tag{14}$$

But

$$\mathfrak{F}\{h\} = \mathfrak{F}\{\mathfrak{F}\{P\}\} = -P \qquad \text{(inverted image)} \tag{15}$$

Substituting (15) into (14)

$$G_i = -P\ G_o \tag{16}$$

So

$$P = \left|\frac{G_i}{G_o}\right| = \text{MTF} \tag{17}$$

Thus it is seen that the pupil function, P, for a coherent system is the MTF. The pupil function, and thus the MTF, for such a system is constant from zero spatial frequency to a cutoff spatial frequency, ν_c, given by:

$$\nu_c = \frac{k\ a}{2\ F} \tag{18}$$

k = wave vector of the light
a = aperature diameter
F = focal length of the mirror

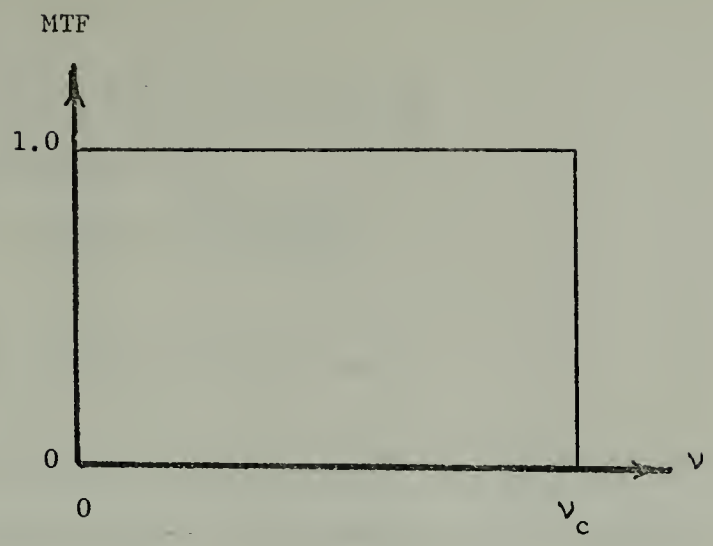

Figure 1. MTF of a Coherent System

2. MTF of a Noncoherent System

In an optical system for noncoherent light the intensity of the image, I_i, is the convolution of the object intensity, I_o, and the square of the point spread function, h; i.e.

$$I_i = |h|^2 * I_o \tag{19}$$

Recall

$$h = \mathfrak{F}\{P\} \tag{8}$$

Thus, from the autocorrelation theorem:

$$|h|^2 = |\mathfrak{F}\{P\}|^2 = \mathfrak{F}\{P(x) * P(-x)\} \tag{20}$$

Substituting into (19)

$$I_i = \mathfrak{F}\{P(x) * P(-x)\} * I_o \tag{21}$$

and taking the Fourier transform of both sides

$$\mathfrak{F}\{I_i\} = \mathfrak{F}\{\mathfrak{F}\{P(x) * P(-x)\} * I_o\} \tag{22}$$

Now, applying the convolution theorem

$$\mathfrak{F}\{I_i\} = \mathfrak{F}\{\mathfrak{F}\{P(x) * P(-x)\}\mathfrak{F}\{I_o\} \tag{23}$$

so

$$\mathfrak{F}\{I_i\} = -\{P(x) * P(-x)\}\mathfrak{F}\{I_o\} \quad \text{(inverted image)} \tag{24}$$

Now if

$$\mathfrak{F}\{I_i\} = G_i \text{ and if } \mathfrak{F}\{I_o\} = G_o \qquad (25\ a,b)$$

Then, substituting into (24)

$$G_i = -\{P(x) * P(-x)\}G_o \qquad (26)$$

and

$$\frac{G_i}{G_o} = -P(x) * P(-x) = MTF \qquad (27)$$

So, it is seen that the MTF of a noncoherent system is the autocorrelation of the pupil function of the system, or the convolution of the aperature with itself.

3. MTF of a Circular Aperature

The optical system used in this project, as are a great majority of optical systems in use today, has a circular aperature. Thus, from the definition of (27), the MTF of a circular aperature is equal to the area of the overlap of the circle, A_o, as it convolves with itself, divided by the area of the aperature, A; i.e.

$$MTF = \frac{A_o}{A} \qquad (28)$$

Clearly, in figure 2, the area of overlap is four times the area of the cross-hatched section, or,

$$A_o = \left[\pi r^2 \cdot \frac{\phi}{2\pi} - \frac{(r \sin \phi)\ (r \cos \phi)}{2}\right] \times 4 \qquad (29)$$

Expanding (29)

$$A_o = \frac{4\pi r^2 \phi}{2\pi} - 2r^2 \sin\phi\cos\phi \qquad (30)$$

and simplifying

$$A_o = 2r^2(\phi - \sin \phi \cos \phi) \qquad (31)$$

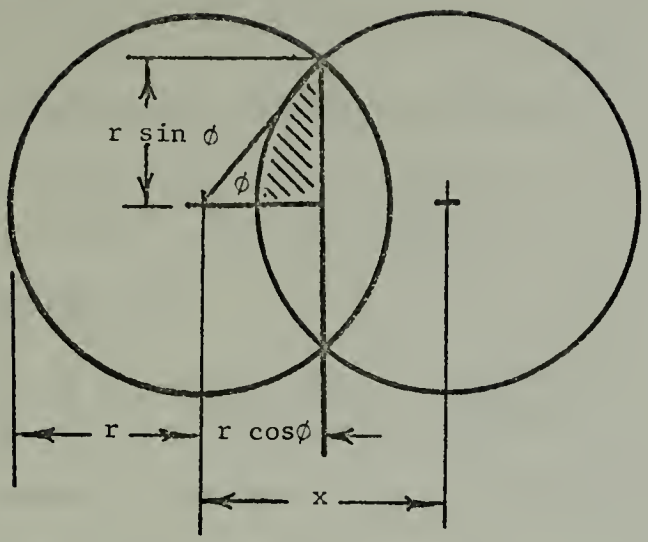

Figure 2. Autocorrelation of the Pupil Function

It is known that

$$A = \pi r^2 \tag{32}$$

therefore, substituting into (28)

$$MTF = \frac{2r^2(\phi - \sin\phi\cos\phi)}{\pi r^2} \tag{33}$$

or

$$MTF = \frac{2\ (\phi - \sin\phi\cos\phi)}{\pi} \tag{34}$$

Calling the maximum spatial frequency, or cutoff frequency, ν_c, then the normalized spatial frequency is

$$\frac{\nu}{\nu_c} = \frac{x}{2r} \tag{35}$$

But

$$\frac{x}{2r} = \cos\phi \tag{36}$$

so

$$\phi = \cos^{-1}\frac{x}{2r} \tag{37}$$

and

$$\sin \phi = (1 - \cos^2 \phi)^{\frac{1}{2}} \text{ or } \sin \phi = (1 - \frac{x^2}{4r^2})^{\frac{1}{2}} \qquad (38\ a,b)$$

Now, substituting (36), (37), and (38b) into (34)

$$\text{MTF} = \frac{2}{\pi}\left[\cos^{-1}\frac{x}{2r} - \frac{x}{2r}(1 - \frac{x^2}{4r^2})^{\frac{1}{2}}\right] \qquad (39)$$

Finally, substituting (35)

$$\text{MTF} = \frac{2}{\pi}\left\{\cos^{-1}\frac{\nu}{\nu_c} - \frac{\nu}{\nu_c}\left[1 - (\frac{\nu}{\nu_c})^2\right]^{\frac{1}{2}}\right\} \qquad (40)$$

When plotted as a function of spatial frequency this MTF curve, (figure 3,) is nearly a straight line at the lower frequencies and has a slope of -4π. But at the higher frequencies the curve loses its slope gradually and moves out to intercept the horizontal axis at the cutoff frequency.

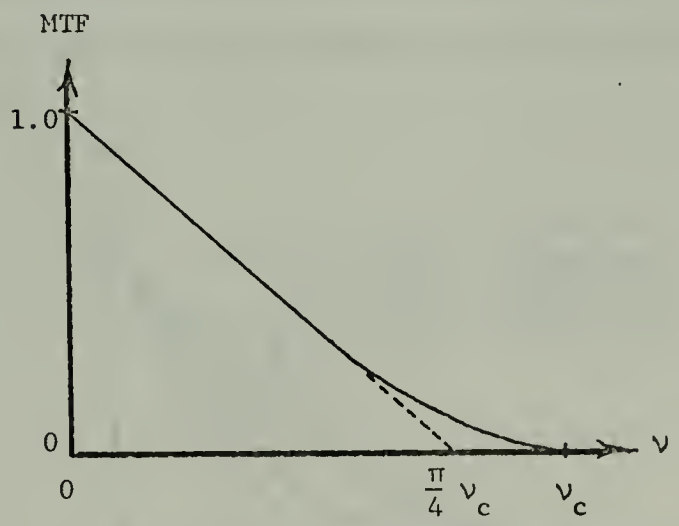

Figure 3. MTF of a Circular Aperture in Noncoherent System

C. DEFOCUSING AND THE MTF CURVE

1. The Effect of Optical Equipment Limitations on MTF

Figure 3 shows the MTF curve for a diffraction limited system. However, most practical systems are limited to some extent by inherent lens or mirror abberations and manufacturing inaccuracies present in the basic optical components. Add to these the limitations of spatial modulation caused by the responsivity time constants and the problems of noise in the system and it becomes obvious that the diffraction limited curve will not always be achieved. Limitations, such as those mentioned above, result in some loss of MTF. This results in an MTF curve that falls below that of the diffraction limited curve. In some cases, for example, for defocusing, the MTF curve will actually fall below the ordinate of the graph. This condition is known as negative MTF. It is recognized optically by a reversal of the true shading in the image. Dark shades turn light and light shading becomes dark when negative MTF is experienced.

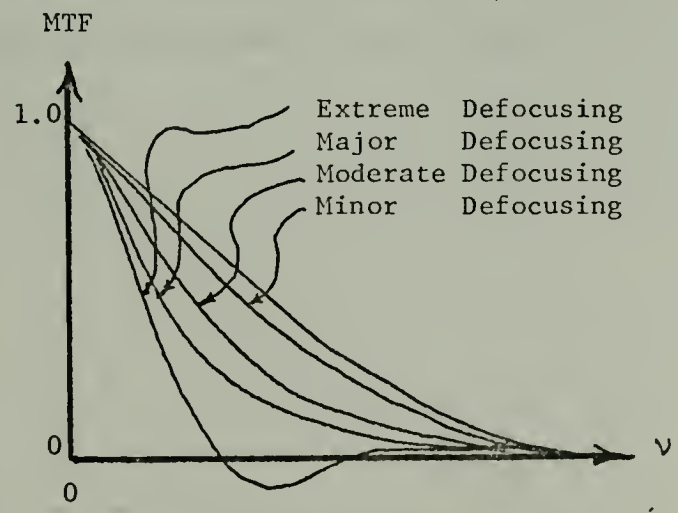

Figure 4. Defocusing Effects on MTF

2. The Effect of Turbulence on MTF

Turbulence in the atmosphere results in changes in the refractive index structure along the line of sight through this medium. Large scale disturbances are of some interest, but disturbances on the order of centimeters are of particular interest to this project. Turbulence of this magnitude, and the resultant structure of the atmospheric refractive index causes instantaneous image degradation with an effect on the MTF curve similar to that caused by the limitations discussed earlier, as well as random image displacement resulting from the changes in the atmospheric refractive index along the line of sight.

Devices are available that will act as probes in the atmosphere and will provide information on microtemperature fluctuations and humidity fluctuations leading toward the measurement of the refractive index structure constant, C_N, discussed by Tatarski. (See Bibliography)

Atmospheric turbulence and resulting microvariations in refractive index profiles tend to introduce phase variations, i.e. incoherence, into beams emanating from the normally coherent light from a laser.

III. THE EXPERIMENT

A. EXPERIMENTAL APPARATUS

To carry out this project it was necessary to produce an optical apparatus with sufficient resolution to provide information on image degradation as a result of turbulence in the atmosphere. The apparatus designed and constructed consisted of a telescope to view the targets under study, a scanning mechanism that would sweep the line of sight across the target of variable intensity, a reticle, or chopper, that would provide an absolute base for irradiance information, electronic display and recording equipment, and targets that were designed to provide luminous fluxes of varying intensity.

1. Optics

A reflector telescope was used to observe a target. A nine inch diameter aluminum tube, six feet long, and painted ultra-flat black on the inside was used as the basic telescope frame. A six inch diameter parabolic mirror with a focal length of five feet was mounted on a three-point (adjustable line of sight) base at one end of the telescope. Fine focusing of the telescope was provided with a micrometer screw controlling the longitudinal position of the mirror base.

A 45^{o} reflecting mirror was mounted on the longitudinal axis of the telescope. The angle of this mirror, (an integral part of the scanning mechanism to be described below,) caused the image to be reflected through an opening in the tube and onto an entrance slit located in the light tight cavity of the monochromator of a Perkin-Elmer model 13 spectrophotometer.

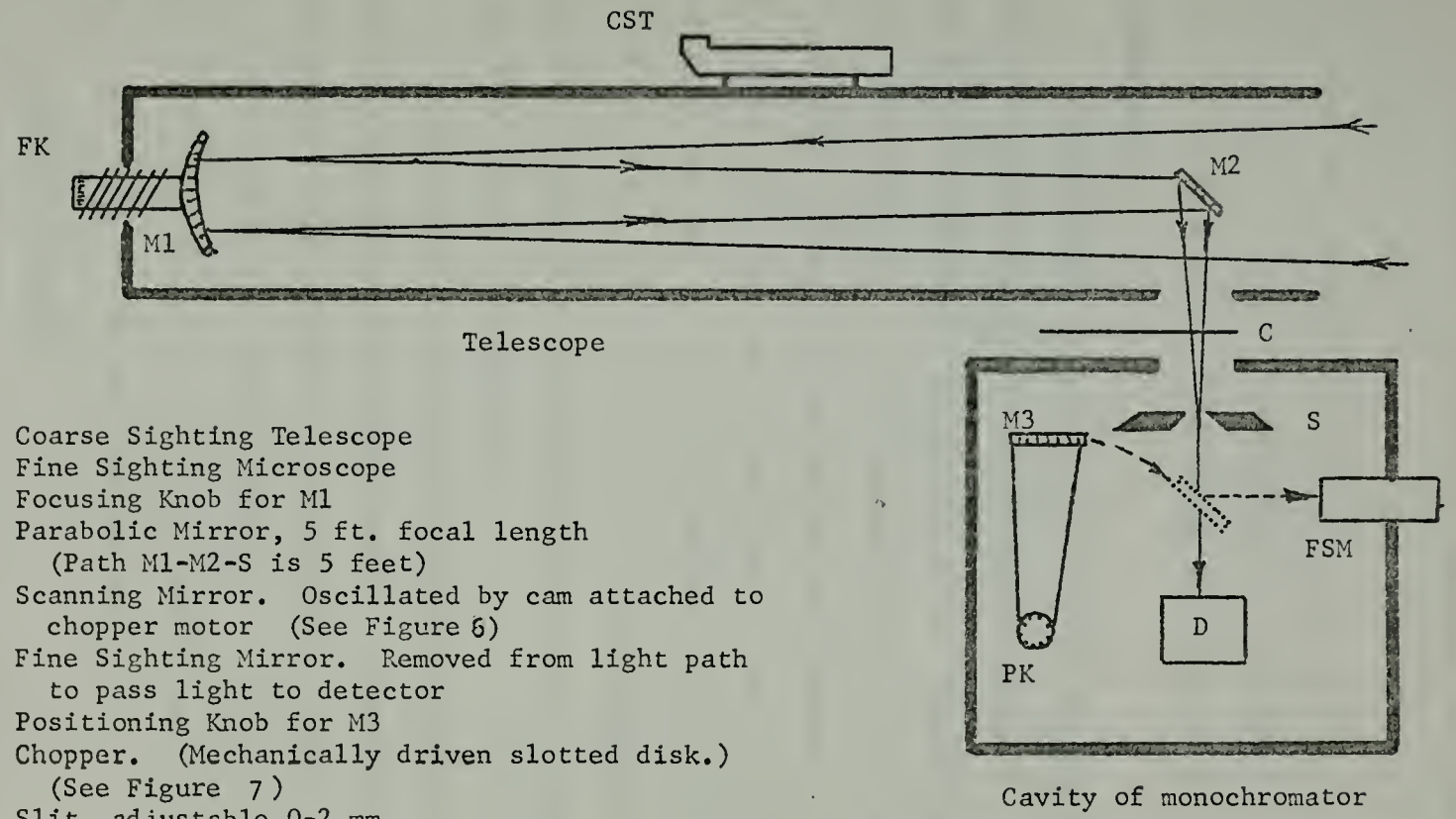

CST: Coarse Sighting Telescope
FSM: Fine Sighting Microscope
FK: Focusing Knob for M1
M1: Parabolic Mirror, 5 ft. focal length
(Path M1-M2-S is 5 feet)
M2: Scanning Mirror. Oscillated by cam attached to chopper motor (See Figure 6)
M3: Fine Sighting Mirror. Removed from light path to pass light to detector
PK: Positioning Knob for M3
C: Chopper. (Mechanically driven slotted disk.) (See Figure 7)
S: Slit, adjustable 0-2 mm
D: Detector

Figure 5. Path of Light Through Telescope to Detector

The parabolic mirror of the telescope, the scanning mirror, and the entrance slit were located in such a manner that the optical path length from the telescope mirror to the entrance slit, via the 90^{o} reflection caused by the 45^{o} scanning mirror was equal to the focal length of the telescope mirror. This caused the image to be focused at the entrance slit.

Initial coarse sighting of the target was accomplished by a small sighting telescope mounted on the main telescope tube. Confirmation of image sighting and image identification were accomplished with the entrance slit adjusted to a wide opening and by a fine sighting mirror that could be rotated into the optical path passing throught the entrance slit. This mirror was mounted on an arm in such a way that it was at 45^{o} when in the line of sight and provided a view of the entrance slit and the telescope image through a microscope that was mounted through the monochromator shell. This view of the slit and image was the same as the view seen by the detector.

Excessive losses suffered by the light passing through the multiple optics of the monochromator resulted in the decision to bypass these optics. Thus the detector was placed directly behind the entrance slit rather than at the designed exit slit. In order to accomodate the detector, it was necessary to remove excessive parts (collimator, thermocouple, exit slit, and prism) from the cavity.

2. Scanning Mechanism

It was necessary to build a mechanism that would provide a line of sight that would sweep across the target into the system. Such a scanning mechanism would permit obtaining the required data on modulation of light from the target. It was done by mounting the 45^{o} scanning

mirror on the longitudinal axis of the telescope by means of a vertical pivot that penetrated the tube. The top of this pivot was fixed to a movable arm that acted as a cam follower. The following action of this arm caused the 45° reflecting mirror to horizontally scan the image of the telescope back and forth across the entrance slit.

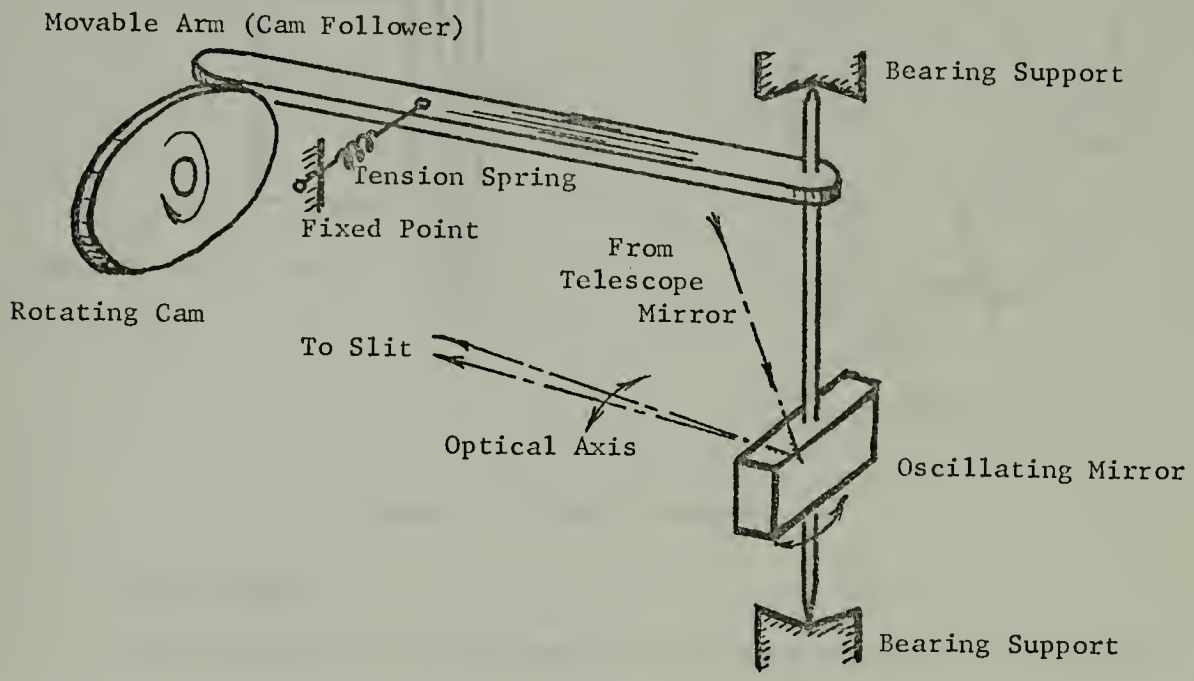

Figure 6. Scanning Mechanism

3. Reticle, (or Chopper)

Interruptions in light passing to the detector will give an absolute 'black' reference. A rotating disc with two chopper blades, the reticle, was fixed so that the chopper rotation resulted in just such short interruptions in light passage through the adjustable entrance slit. A cam was mounted on the axis of the chopper drive motor and reticle disc to provide scanning action for the scanning mirror, as described above. The cam was of an elliptical shape the resulted in two image scanning periods for each revolution of the chopper. The two blades of

the reticle and proper alignment of the cam on its axis provided for a chop, or 'black' reference, at the beginning and end of each scanning period.

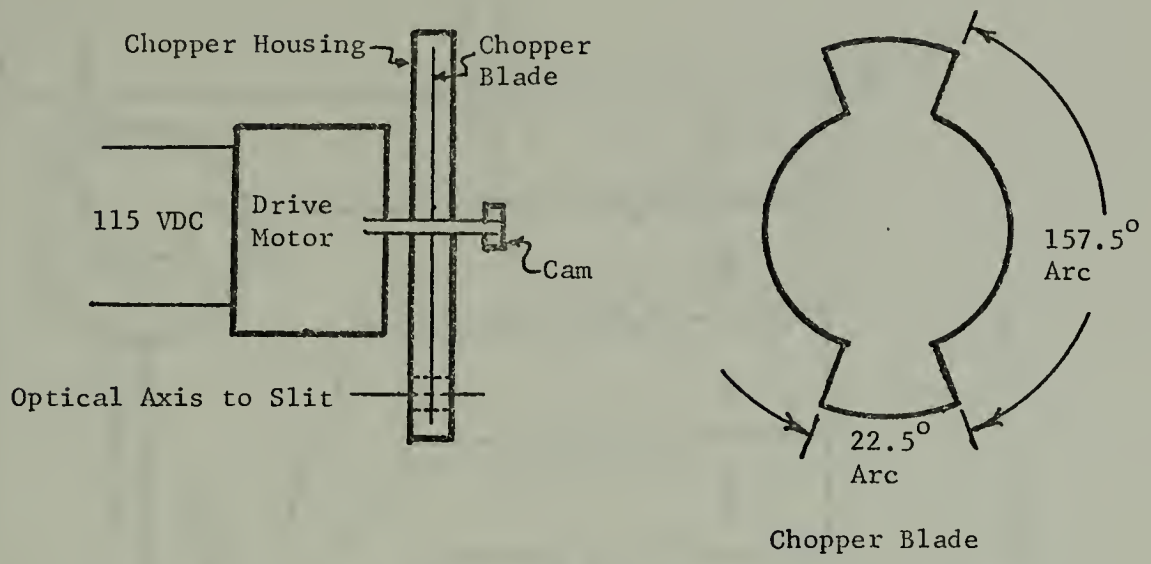

Figure 7. Chopper Mechanism

4. The Detector

The detector assembly, figure 8, was based on an E G & G Incorporated type SGD-444 silicon photodiode detector and an N channel type 2N3819 field effect transistor (FET) used as a "source follower" to match the high impedance of the photodiode circuit to the 50 ohm cable to the oscilloscope. This reduces "pickup" noise. The FET was provided with a +9VDC drain voltage producing a 0.35 ma drain current. Two outputs for the electrical signal voltage were available. The first was across a 10K ohm follower resistor connected to the source. The second was across a resistor, (or open circuit,) connected to the gate of the FET. This resistance was variable from 10 ohms to 10 megohms in decade steps. These variable resistances in the gate circuit provided some flexibility in selecting between strength of signal and response time of the circuit.

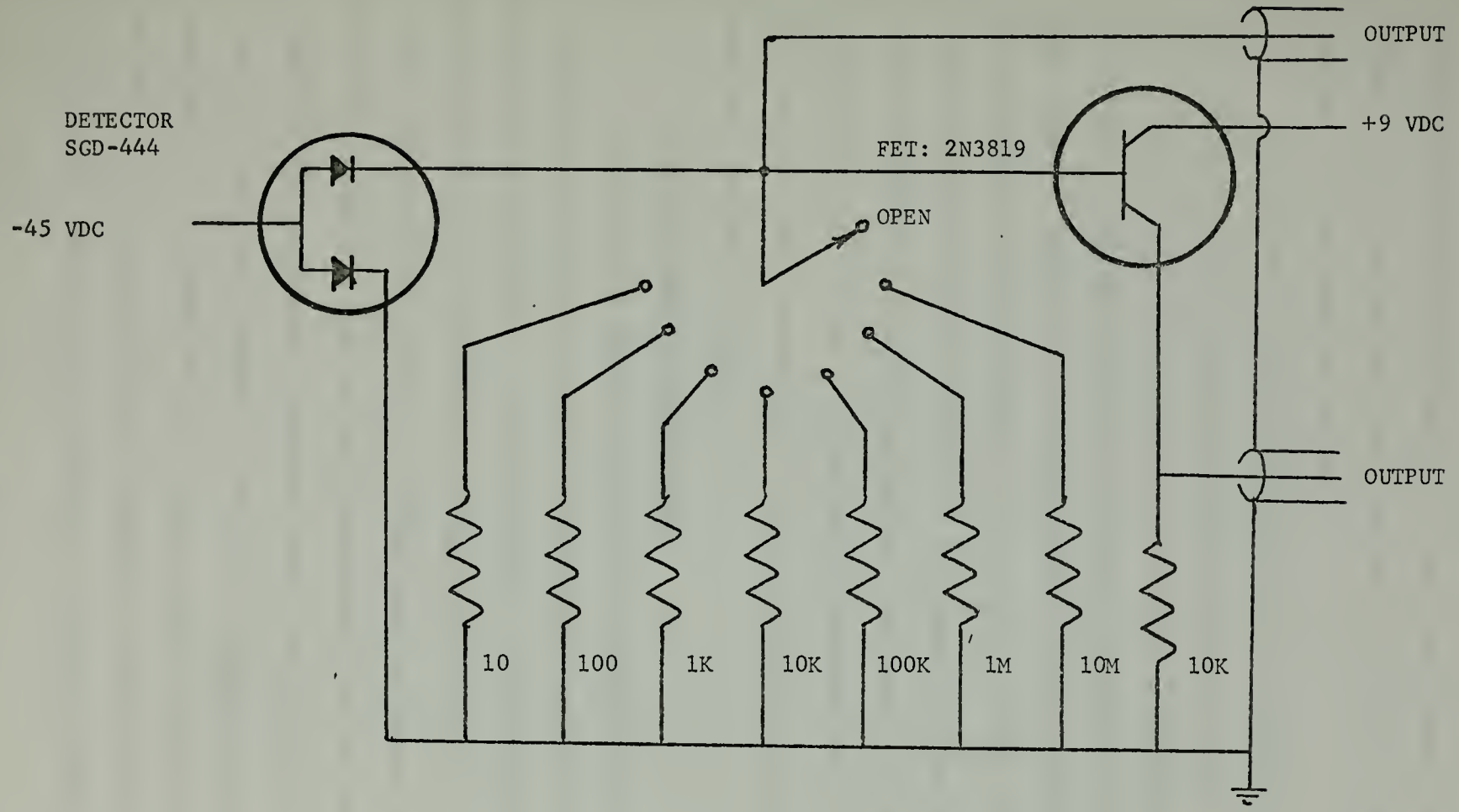

Figure 8. Schematic of Detector Circuit

The best compromise between a strong signal and a short response time for the scan rate used, (approximately 30 sweeps each second,) was with the output taken across the gate resistance which was set at 100K. The silicon detector was biased at −45 VDC.

The detector circuitry was mounted in a shielded box that was initially made fast to the base of the monochromator cavity. However, it was noticed that acoustic vibrations from the cam/chopper operations were picked up microphonically in the detector circuitry resulting in a high frequency overlay on the detected signal. This problem was reduced by placing the detector assembly in the cavity on a foam rubber pad and by fine adjustments to the bearings of the scanning mechanism pivots. It is recommended that any future devices constructed for similar work be designed in such a way as to physically locate the detector circuitry in a position that is mechanically isolated from any vibrating equipment associated with the apparatus.

5. Electronic Display and Recording

The electrical signal voltage from the detector was fed to a Tektronix type 1A7 plug-in differential amplifier and a Tektronix type 551 dual beam oscilloscope. This provided for visual orientation by the operator. This same signal was taken from the amplifier output and fed to a Princeton Applied Research (PAR) model 160 boxcar integrator. The boxcar integrator took the amplified signal from the detector and integrated the continuously repeating signal over a period of time. As a result of this time integration random noise effects were reduced by a large factor. It should be kept in mind, however, that the integration process will not remove noise of a repetative nature, such as acoustic coupling. Only random noise is reduced. A Hewlett - Packard model

7035B X-Y recorder converted the output of the boxcar integrator into a permanent graphic recording of the electrical signal, (less random noise,) from the detector. This graphic recording could then be accurately analyzed at leisure. Figure 9, on the following page, is a block diagram of the entire detection and recording system used in this project.

6. Oscilloscope Trace Synchronization

Modulation of the signal at the higher spatial frequencies used was quite small and all signals were subject to a great deal of noise. These conditions resulted in a marked degree of undependability in the use of signal self triggering of the oscilloscope. Because of this and the resultant difficulty in preventing overlapping and non-synchronized traces of the electrical signal it was decided to mate the signal from the detector to a trigger/synchronizing pulse generated by the chopper blades.

A small magnet and soft iron core coil were clamped into position on opposite sides of the aluminum chopper housing. The magnetic field of the magnet tended to cross the point of passage of the chopper blade and concentrate in the iron core of the coil. The magnet/coil positions were diametrically opposite the position of the openings to the entrance slit at the base of the chopper housing. As the spinning chopper blades moved in the magnetic field their eddy currents affected the strength of the magnetic field in the core of the coil. The resulting change in magnetic flux through the core caused an inductive voltage in the coil itself. When the chopper blade was up to speed, the induced voltage, fed through a Tektronix type E plug-in amplifier serving the second beam of the dual beam oscilloscope, was of sufficient strength to trigger the oscilloscope. The location of the magnet/coil and chopper performing

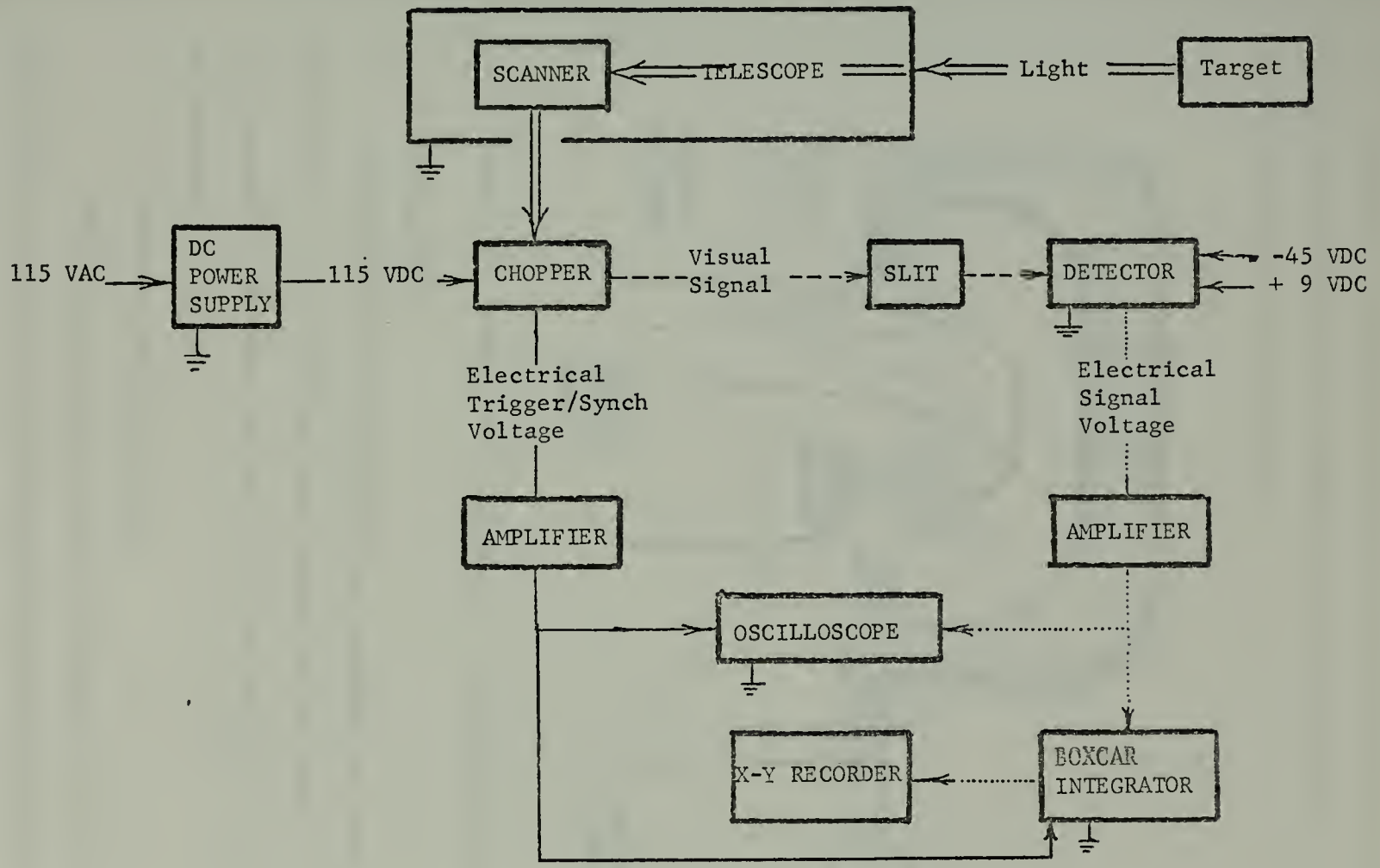

Figure 9. Block Diagram of Detection and Recording System

this function, diametrically opposite the blade actually performing the optical chop at this time, insured that the trigger pulse would be properly synchronized with each chop.

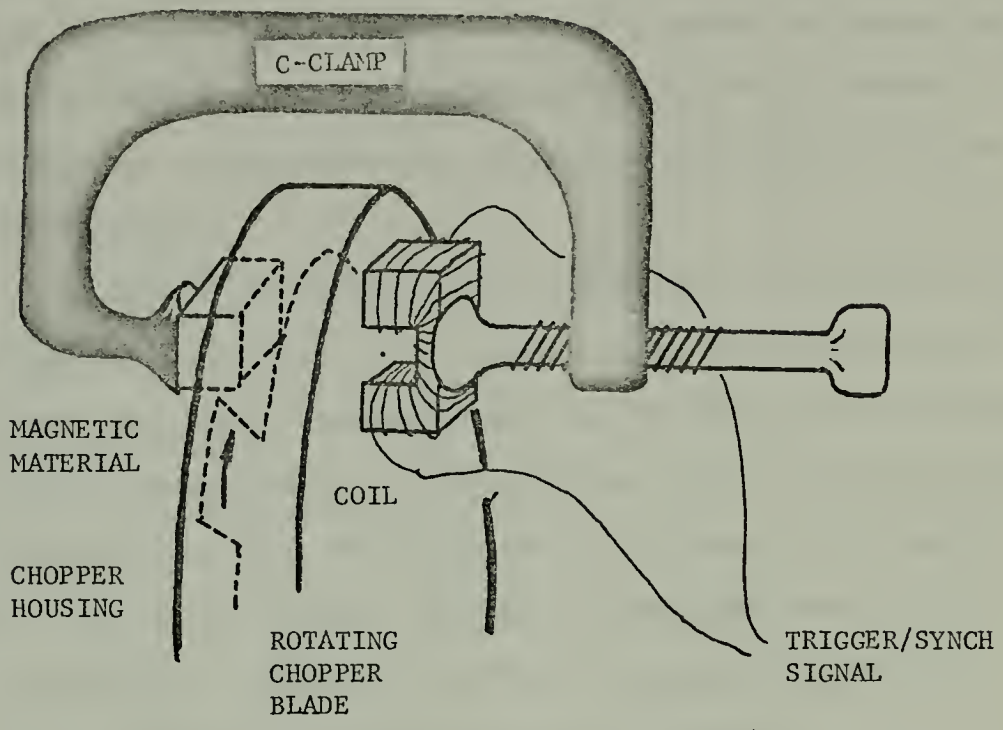

Figure 10. Mechanism for Generation of Trigger/Synch Pulse

7. Test Targets

Targets used for this project were designed to give a periodic modulation of the optical wave when scanned by the system. They consisted of vertically arranged stripes of periodic intensity easily sighted and horizontally scanned.

a. Black and White Bar Chart

The target initially used consisted of an 8' x 4' plywood panel painted flat black. On this panel were mounted vertical strips of white, beaded picture projector screen. Each strip was ten centimeters in width and spaced ten centimeters from the adjacent white strip.

This provided an alternating black/white target with a spatial frequency of five cycles, (line pairs,) per meter.

This target produced a display of repeating pedestals. The high frequency components of a periodic step function were beyond the bandwidth of the electronic equipment used. As a result the display had rounded rather than square corners. This was not a problem, however, since the interest of the project was directed at the amplitudes of the fundamental frequency.

By opening the image plane slit from 0.1 mm to 0.4 mm a much stronger signal was generated by the detector. The signal then became a periodic trapezoid, and a triangular signal at the higher spatial frequencies. Slope was introduced to the periodic functions by the time-varying change in light detected by the photodiode as the image of the edges of the target swept across the slit. The diffraction limit would correspond to a slit width of .005 mm. The MTF of the instrument was thus limited by the slit width at the higher spatial frequencies, but the resolution was still high enough to detect the effects of the atmospheric turbulence.

b. Sinusoidal Intensity Chart

An improved target provided a pure spatial frequency capable of being reproduced on the display was made by programming a Hewlett - Packard model 9810A calculator, which was used in conjunction with the model 9862A calculator-plotter, to produce a graphical chart consisting of small, (smaller than the resolution of the optical equipment,) vertical chart lines spaced at distances which were proportional to the sine of the ordinate. (The program for such a target graph is included as Appendix A.) The appearance of this target as seen by the detector

is a pure spatial frequency varying in reflectivity proportional to $\sin^2$ of the horizontal axis from white, to gray, to black, to gray to white, then repeating periodically.

The display of signal voltage from such a target was a sine wave. However this target lacked intensity as the paper has small reflectivity and the ink which produced the dark portions of the chart was not highly absorbent. It is considered that a target providing a much more intense, and therefore desirable, pattern could probably be produced with paint that is shaded gradually and sinusoidally from gloss white to flat black, etc.

B. TESTING THE APPARATUS

Initial tests of the apparatus were conducted in the basement corridor of Spanagel Hall at the Naval Postgraduate School in Monterey, California. This location provided a distance of 135 meters between the target and the parabolic mirror of the telescope. The target used was the black and white vertical bar chart. Normal basement illumination consisted of 60 cycle fluorescent tube arrays spaced periodically throughout the basement. This resulted in a flashing illumination of the target which was unacceptable, (but would not be found in natural outdoor lighting by the sun.) This variable illumination was countered by turning off most of the offending lights, (safety circuits prevented complete turning off all of these lights and plunging the entire corridor into an unsafe condition of total darkness,) and illuminating the target with a 6VAC motion picture projector incandescent lamp. This lamp was placed in a lensed casing that projected a circular beam of noncoherent light on the bar chart. Because of the short distance from the lamp to the target, which prevented sufficient spread of the illuminating beam, the illuminance,

(luminous flux per unit area,) of the target was less at the outer edges of the lamp's beam and greatest at the center of the beam.

The telescope was positioned on target with the coarse sighting telescope, and eased into final position with the fine sighting microscope. While observing the target through the fine sighting microscope the chopper disc was rotated slowly by hand. While doing this the operator was able to observe the image being chopped, then scanned for a full cycle, and finally chopped again. This procedure permitted absolute identification of the target image and proper orientation by the operator. This leads to a good interpretation of the oscilloscope display.

The figures on the following page show a complete cycle of the scanning mechanism; the path across the target from chop to chop, the resultant oscilloscope display, and interpretation of the display.

Light meter readings of the illuminated target in the basement location were compared with readings on the target taken in natural light outside. The light meter used was an ordinary and simple photographic light meter which provided recommended shutter speeds at any given f-stop for a film of a particular ASA index. In this case the meter recommended an exposure of 30 seconds for f/11 for the bar chart in the basement and 1/15 second outside in total shade under a hazy sky. This is a ratio of 450:1. In direct sunlight under hazy skies the lightmeter recommended an exposure of 1/125 second. This is a ratio of 3750:1. Such results would indicated that intensity of signal from the target located outside would be from approximately two to approximately four orders of magnitude greater than in the basement location. This would greatly increase the signal-to-noise ratio for out-of-door operation of the apparatus.

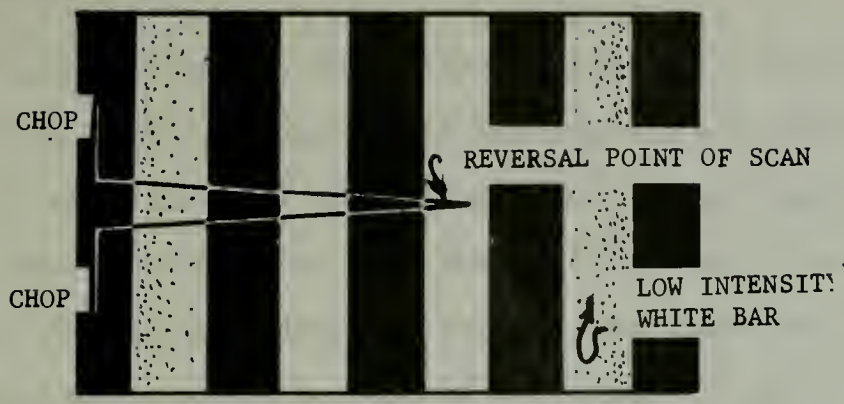

Figure 11. Typical Scanning Path Over Bar Chart

Figure 12. Typical Oscilloscope Display of Signal Detected from Scanning Bar Chart

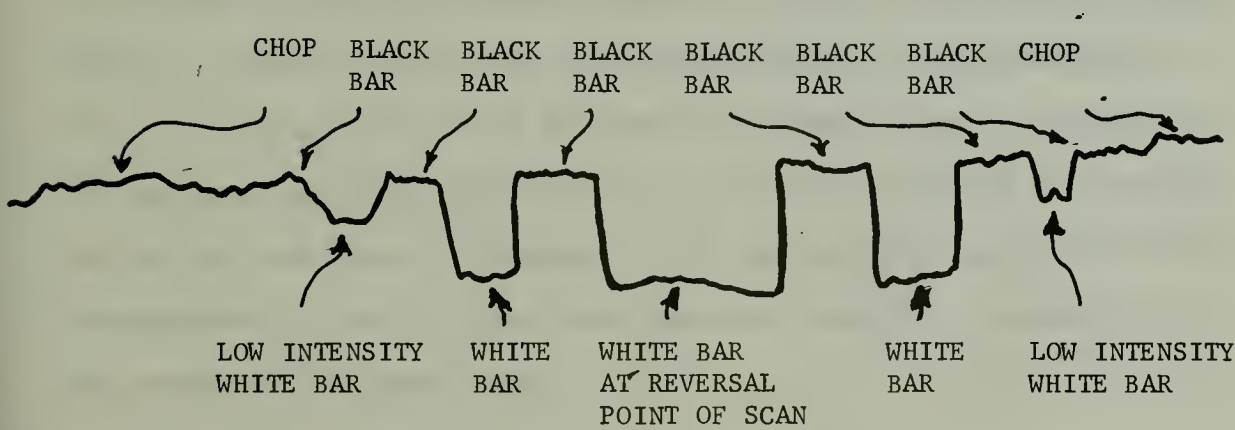

Figure 13. Interpretation of Oscilloscope Display

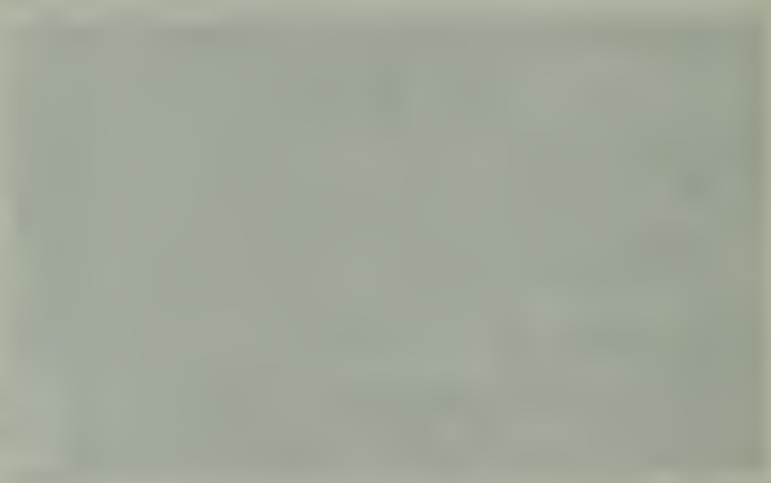

C. TESTING FOR TURBULENCE

The basement corridor is ventilated by a system of seven overhead blower outlets located at regular intervals but with some variation in height and freedom from flow obstruction. A helium-neon laser from C W Radiation, Incorporated, producing a beam at 6328Å, was set up at the location of the telescope, defocused somewhat, and beamed at a plane, face-silvered mirror at the location of the target. It reflected its beam on a white paper screen located above the telescope. In the 270 meter path to the mirror and returning, the defocused laser beam observed on the screen was seen, quite readily, to be undergoing scintillation, or turbulence effects with the blowers running. When the blowers were stopped and the air in the corridor allowed to settle the observed scintillation was greatly reduced.

In order to estimate the amount of turbulence present the detector was removed from the monochromator cavity and placed in the reflected and defocused beam of the laser. The output of the Tektronix type 1A7 differential amplifier, to which the detector was connected, was fed to a type 1564-A sound and vibration analyzer produced by the General Radio Company. Results of this test indicated that there was approximately 50 per cent modulation of the beam when the blowers were on compared to two per cent modulation with the blowers turned off and the air settled. The obvious conclusion: turbulence in the testing area can be varied from considerable to light. These conditions were found to be suitable for the conduct of the experiment.

D. CONDUCT OF THE EXPERIMENT

With the blowers turned on, the target was illuminated with the 6VAC lamp, the telescope was sighted in and focused on the target, and the target was scanned. Target modulation graphs were obtained for the spatial frequency of the target. The spatial frequency of the observed target, ν, was equal to:

$$\nu = \frac{\nu_t}{\sin \theta} \qquad (41)$$

ν_t = spatial frequency of the face of the target

θ = angle between the line of sight and the face of the target

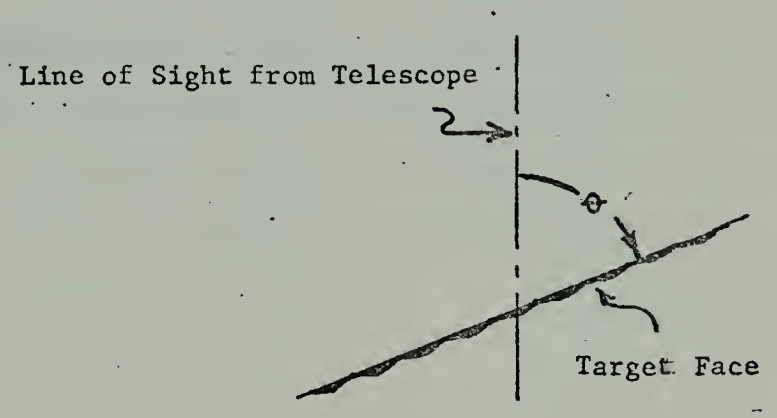

Figure 14. Determination of Spatial Frequency of Observed Target

Once a graph was obtained the value of θ was altered, thus causing a change in the spatial frequency of the observed target. A series of such graphs was obtained. The blowers were shut off, the corridor air allowed to settle, and the same procedure was repeated using the same values of θ.

The MTF of each modulation graph was then calculated and plotted on graphs of spatial frequency versus MTF for each blower status. The curves were extrapolated to the abscissa to determine MTF at zero cycles. This value was used to normalize the MTF curves.

Data from the experiment and the calculated values of MTF are included as Appendix B. The curves of MTF (observed) are presented as Appendix C. The curves of MTF (normalized) are presented as Appendix D.

E. RESULTS OF THE EXPERIMENT AND CONCLUSIONS

MTF curves plotted, (Appendix D,) indicate that there is a degradation of the image of the optical system described as a result of the microturbulences caused by normal operation of the building's ventilation system, and that the optical apparatus used was successful in detecting the effect of these microinstabilities on MTF. Reduction of MTF appears to be inversely proportional to the spatial frequency observed. Using an apparatus such as this, in conjunction with an available system for thermal C_N measurement could provide a technique to quantify the effect of atmospheric turbulence on the MTF of a spatially modulated optical transmission through the atmosphere.

APPENDIX A

Computer Program for Sinusoidal Intensity Bar Chart (Interlaced Scanning) Using the Hewlett-Packard 9810A Calculator in Conjunction with the Hewlett-Packard 9862A Calculator Plotter

```
0000--CLR---20
0001--  1  --01
0002--  0  --00
0003--  0  --00
0004--  0  --00
0005--FMT---42
0006--  UP--27
0007--XEY---30
0008--  8  --10
0009--  0  --00
0010--  0  --00
0011--  1  --01
0012--XEY---30
0013--FMT---42
0014--  DN--25
0015--RUP---22
0016--  2  --02
0017--  0  --00
0018--  0  --00
0019--  0  --00
0020--  +  --33
0021--  0  --00
0022--XEY---30
0023--FMT---42
0024--  UP--27
0025--CHT---47
0026--RUP---22
0027--XEY---30
0028--FMT---42
0029--  DN--25
0030--XEY---30
0031--  0  --00
0032--  0  --00
0033--  4  --04
0034--  1  --01
0035--RUP---22
0036--GTO---14
0037--  0  --00
0038--  0  --00
0039--  1  --01
0040--  0  --00
0041--CHT---47
0042--CHT---47
0043--CHT---47
0044--CHT---47
0045--CHT---47
0046--CHT---47
0047--CHT---47
0048--CHT---47
0049--CHT---47
0050--CHT---47
0051--  r  --56
0052--RUP---22
0053--  2  --02
0054--  0  --00
0055--  0  --00
0056--  0  --00
0057--DIV---35
0058--  t  --14
0059--  X  --36
0060--XEY---30
0061--  N  --70
0062--  UP--27
0063--  X  --36
0064--  .  --21
0065--  9  --11
0066--  X  --36
0067--  1  --01
0068--XEY---30
0069--  -  --34
```

```
0070--  1  ----01
0071--  5  ----05
0072---XEY-----30
0073---DIV-----35
0074--  t  ----14
0075--  +  ----33
0076---XEY-----30
0077--XTO-----23
0078--  t  ----14
0079--CMT-----47
0080---RUP-----22
0081---EEX-----26
0082--  3  ----03
0083--  +  ----33
0084--  0  ----00
0085---XEY-----30
0086--FMT-----42
0087--  UP----27
0088---XEY-----30
0089--  8  ----10
0090--  0  ----00
0091--  0  ----00
0092--  1  ----01
0093--XEY----30
0094--FMT----42
0095--  DN----25
0096--RUP----22
0097--  2  ----02
0098--  0  ----00
0099--  0  ----00
0100--  0  ----00
0101--  +  ----33
0102--  0  ----00
```

```
0103--XEY----30
0104--FMT----42
0105--  UP----27
0106--RUP----22
0107--XEY----30
0108--FMT----42
0109--  DN----25
0110--X>Y----53
0111--  0  ----00
0112--  1  ----01
0113--  2  ----02
0114--  1  ----01
0115--RUP----22
0116--GTO----44
0117--  0  ----00
0118--  0  ----00
0119--  9  ----11
0120--  7  ----07
0121--  t  ----14
0122--CHS----32
0123--XTO----23
0124--  t  ----14
0125--XEY----30
0126--  0  ----00
0127--X>Y----53
0128--  0  ----00
0129--  0  ----00
0130--  8  ----10
0131--  1  ----01
0132--GTO----44
0133--  0  ----00
0134--  0  ----00
0135--  5  ----05
0136--  1  ----01
0137--STP----41
0138--END----46
```

APPENDIX B

Sample Data and Calculated Data

θ	ν	Relative MTF (observed)		MTF (normalized)	
	$\nu = \frac{\nu_t}{\sin \theta}$	blowers on	blowers off	blowers on	blowers off
degrees	line pairs/m				
90	5	.805	.932	.671	.776
45.6	7	.804	.890	.670	.742
30	10	.667	.720	.555	.600
20.9	14	.467	.483	.388	.403
15.3	19	.353	.364	.296	.305
12.03	24	.183	.222	.152	.185

APPENDIX C

GRAPH OF RELATIVE MTF (OBSERVED) AS A FUNCTION OF SPATIAL FREQUENCY

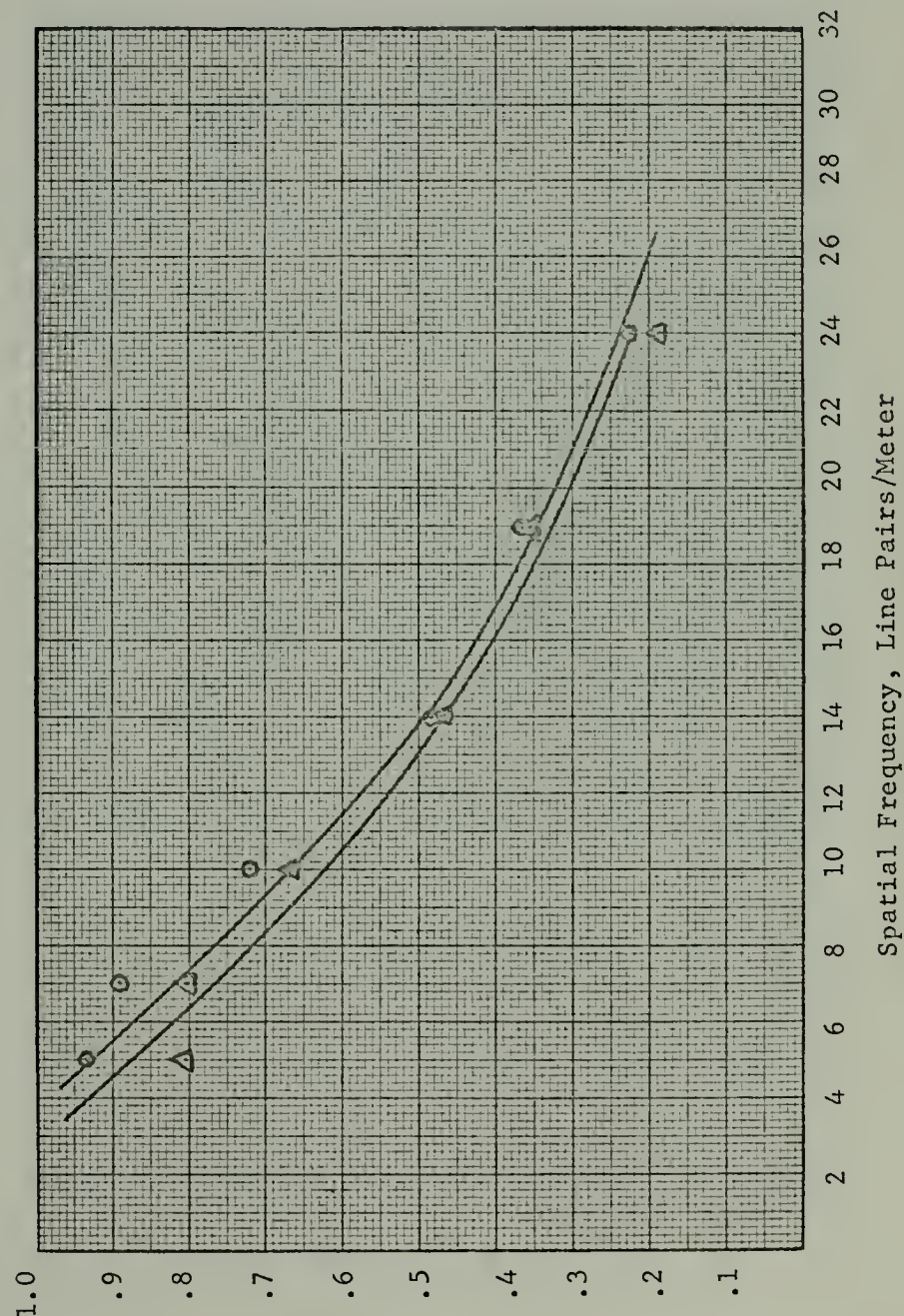

APPENDIX D

GRAPH OF MTF (NORMALIZED) AS A FUNCTION OF SPATIAL FREQUENCY

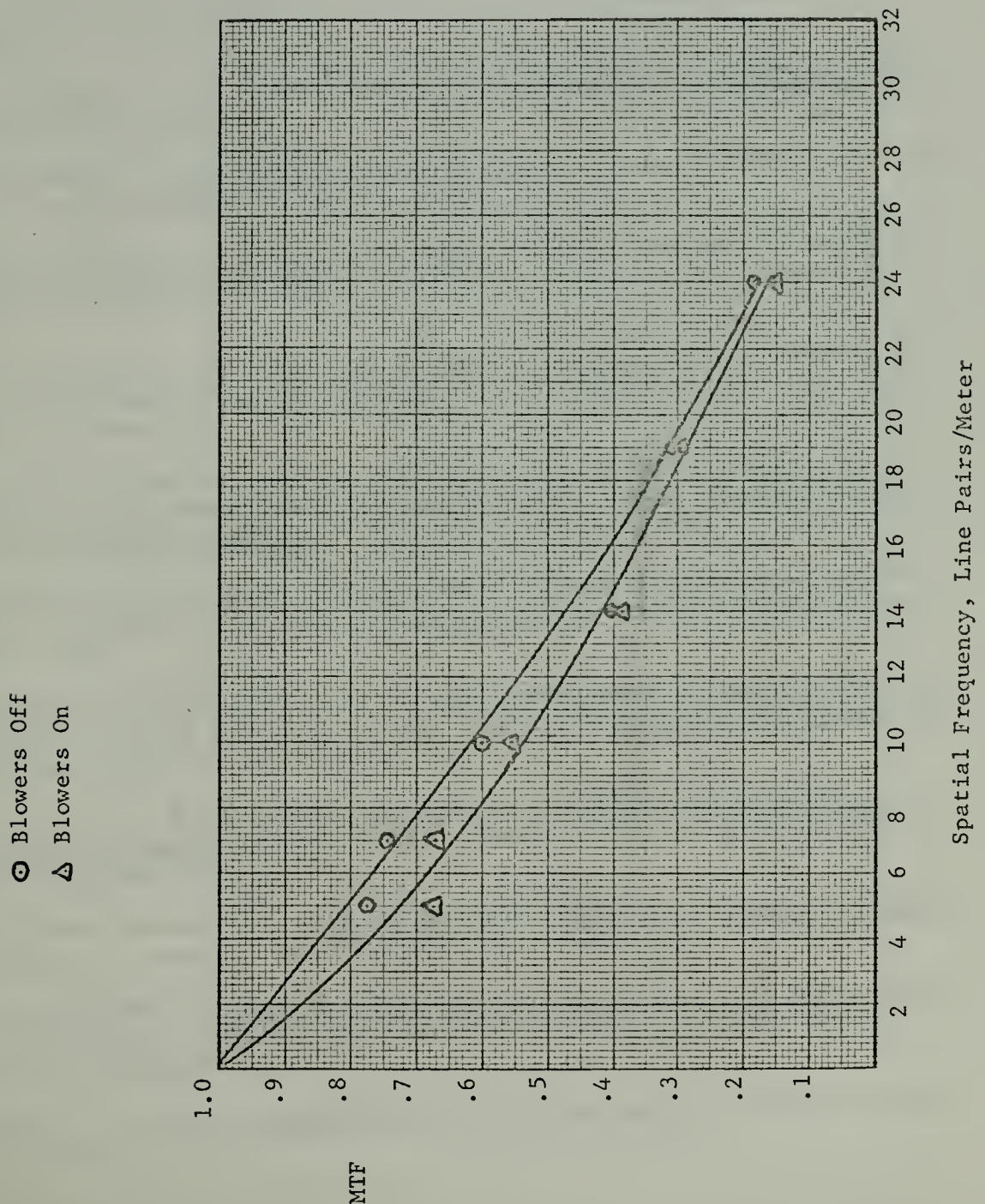

BIBLIOGRAPHY

Bracewell, Ron, The Fourier Transform and its Application, McGraw-Hill Electrical and Electronic Engineering Series. p 24-45. San Francisco: McGraw-Hill, 1965.

Crittenden, Eugene C., Jr., Unpublished lecture notes, Naval Postgraduate School, Monterey, 19 November 1971.

_____. Unpublished lecture notes, Naval Postgraduate School, Monterey, 16 August 1972.

E G & G Incorporated, Data Sheet 013A, SGD-444 Series Silicon Photodiodes, E G & G Inc., Boston.

Fowles, Grant R., Introduction to Modern Optics, p 106, 114-137. San Francisco: Holt, Rinehart and Winston, 1968.

Goodman, Joseph W., Introduction to Fourier Optics, McGraw-Hill Physical and Qunatum Electronics Series. p 110-130. San Francisco: McGraw-Hill, 1968.

Hudson, Richard D., Jr., Infrared System Engineering, Wiley Series in Pure and Applied Optics. p 194, 224-230, 235-261, 266-271. New York: John Wiley and Sons, 1969.

Hufnagel, R. E. and Stanley, N. R., "Modulation Transfer Function Associated with Image Transmission through Turbulent Media," Journal of the Optical Society of America, v 54, p 52-61, January 1964.

Livingston, P.M., "A Study of Target Edge Response Viewed through Atmospheric Turbulence Over Water," Applied Optics, v 11, p 2352-2357, October, 1972.

Lutomirski, R. F. and Yura, H. I., "Modulation Transfer Function of an Optical Wave in a Turbulant Medium," Journal of the Optical Society of America, v 59, p 999-1000, August 1969.

Mackin, Jere G., The Wavelength Dependence of the Modulation Transfer Function of the Atmosphere, Master's Thesis, Naval Postgraduate School, Monterey, June 1972.

Perkin-Elmer Corporation, Instruction Manual, Perkin-Elmer Infrared Equipment, v 3C, Norwalk, Conn.: Perkin-Elmer Corp., 1955.

Schwartz, Mischa, Information Transmission, Modulation, and Noise, McGraw-Hill Electrical and Electronic Engineering Series, p 21-27, 89-102. New York: McGraw-Hill, 1959.

Tatarski, V. I., Wave Propagation in a Turbulent Medium, New York: McGraw-Hill, 1961.

INITIAL DISTRIBUTION LIST

		No. copies
1.	Defense Documentation Center Cameron Station Alexandria, Virginia 22314	2
2.	Library, Code 0212 Naval Postgraduate School Monterey, California 93940	2
3.	Professor E. C. Crittenden, Jr., Code 61Ct (thesis advisor) Department of Physics and Chemistry Naval Postgraduate School Monterey, California 93940	1
4.	LCDR Wayne T. Hildebrand, USN (student) 20270 Anza Dr. Salinas, California 93901	1

UNCLASSIFIED

Security Classification

DOCUMENT CONTROL DATA - R & D

(Security classification of title, body of abstract and indexing annotation must be entered when the overall report is classified)

ORIGINATING ACTIVITY (Corporate author)

Naval Postgraduate School

Monterey, California 93940

2a. REPORT SECURITY CLASSIFICATION

Unclassified

2b. GROUP

REPORT TITLE

An Optical Apparatus to Determine the Effect of Turbulence on the Modulation Transfer Function of the Atmosphere

DESCRIPTIVE NOTES (Type of report and, inclusive dates)

Master's Thesis; (December, 1972)

AUTHOR(S) (First name, middle initial, last name)

LCDR Wayne Thompson Hildebrand, USN

REPORT DATE	7a. TOTAL NO. OF PAGES	7b. NO. OF REFS
December, 1972	44	13

CONTRACT OR GRANT NO.

PROJECT NO.

9a. ORIGINATOR'S REPORT NUMBER(S)

9b. OTHER REPORT NO(S) (Any other numbers that may be assigned this report)

DISTRIBUTION STATEMENT

Approved for public release; distribution unlimited

SUPPLEMENTARY NOTES

12. SPONSORING MILITARY ACTIVITY

Naval Postgraduate School

Monterey, California 93940

ABSTRACT

An apparatus was designed and constructed to determine the effect of atmospheric turbulence on the modulation transfer function (MTF) of the atmosphere. A reflecting telescope and reticle system provided optical information in the visible region to a silicon photodiode detector which was responsive from .35 micron to 1.1 microns. The output of the detector was processed to measure irradiance modulation from a target of known spatial frequency. The modulation transfer function of the atmospheric transmission medium and the optical system was measured under calm conditions and conditions of turbulence on a 270 meter round trip path through a building corridor. The optical apparatus described was capable of detecting, in the visible range, the degrading effect of turbulence on MTF. All reflective optics were used so that the visual through 10 micron range can be covered with use of different detectors.

DD FORM 1 NOV 68 1473 (PAGE 1)

S/N 0101-807-6811

UNCLASSIFIED

Security Classification

A-31408

KEY WORDS	LINK A		LINK B		LINK C	
	ROLE	WT	ROLE	WT	ROLE	WT
ATMOSPHERIC OPTICAL EFFECTS						
ATMOSPHERIC OPTICS						
OPTICAL MODULATION						
MODULATION TRANSFER FUNCTION						
TURBULENCE OPTICAL EFFECTS						
MTF						

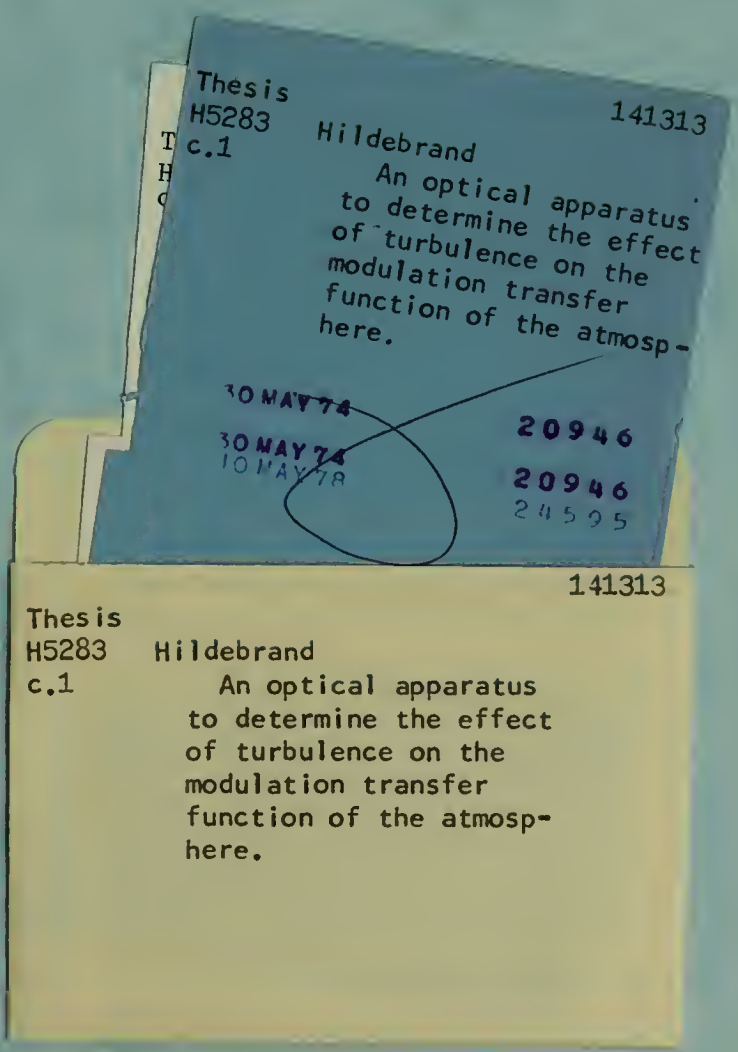

Thesis
H5283 Hildebrand
c.1 An optical apparatus to determine the effect of turbulence on the modulation transfer function of the atmosp-
here.

thesH5283
An optical apparatus to determine the ef
3 2768 002 06036 0
DUDLEY KNOX LIBRARY